Circuit Models for Power Bus Structures on Printed Circuit Boards Using a Hybrid FEM-SPICE Method

Chunlei Guo, *Member, IEEE,* and Todd H. Hubing, *Fellow, IEEE*

***Abstract*—Power bus structures consisting of two parallel conducting planes are widely used on high-speed printed circuit boards. In this paper, a full-wave finite-element method (FEM) method is used to analyze power bus structures, and the resulting matrix equations are converted to equivalent circuits that can be analyzed using SPICE programs. Using this method of combining FEM and SPICE, power bus structures of arbitrary shape can be modeled efficiently both in the time-domain and frequency-domain, along with the circuit components connected to the bus. Dielectric loss and losses due to the finite resistance of the power planes can also be modeled. Practical examples are presented to validate this method.**

***Index Terms*—Finite-element method (FEM), modeling, SPICE.**

I. Introduction

A SUDDEN change in the current drawn by active components on a printed circuit board (PCB) can result in high-frequency voltage fluctuations known as delta-I noise or simultaneous switching noise. This noise may propagate throughout the power bus, causing signal integrity (SI) problems or radiated electromagnetic interference (EMI). In order to mitigate this noise effectively, it is helpful to model both the circuit components and the power bus structure.

In high-speed PCBs, the power is often distributed on closely spaced parallel conducting planes. In recent years, full-wave numerical methods such as the finite-element method (FEM), the finite-difference time-domain (FDTD) and the method of moments (MoM) have been used to analyze parallel-plane power bus structures [1]–[3]. Passive lumped components such as resistors, inductors, and capacitors can generally be incorporated into full-wave numerical methods. However, the active devices or nonlinear components that are often found on populated printed circuit boards are not readily modeled by full-wave methods.

Cavity models have been widely used to analyze parallel-plane structures [4]–[6]. However, cavity models place certain restrictions on the geometries that can be modeled and the complexity of a cavity model analysis increases sharply with the number of components connected to the PCB.

Partial equivalent circuit (PEEC) methods may be used to derive an equivalent circuit network for power bus structures [3]. PEEC methods employ a SPICE-like circuit solver making them well suited for modeling populated boards. However, the resulting equivalent circuit networks have many components due to the dense nature of the matrix equation utilized to generate the equivalent circuits.

Guillouard *et al.* and Feliziani and Maradei demonstrated a technique for analyzing microwave circuits (such as microstrip lines and parallel plate waveguides) using FEM to generate an equivalent circuit network [7]–[9]. In this paper, an FEM formulation is used to derive circuit models that take advantage of the symmetric nature of the FEM matrix to reduce the total number of components. This technique is employed to develop efficient circuit models for PCB power bus structures. Practical issues of employing these circuit models in various situations are discussed. This method of converting the FEM matrix equation into an equivalent circuit and using SPICE to analyze it is referred as FEM-SPICE in this paper.

In Section II, the FEM matrix equation is reformulated to derive an equivalent circuit network. Section III describes the incorporation of various losses into the equivalent circuit network, and practical issues associated with analyzing the equivalent circuit network in a SPICE program are discussed. Numerical examples are provided to validate the FEM-SPICE method and demonstrate its efficiency in Section IV. Finally, conclusions are drawn in Section V.

II. Formulation

The FEM method is well suited for modeling complex, inhomogeneous structures. This section describes how an FEM formulation is converted into an equivalent circuit that can be solved using a SPICE program.

A. FEM Matrix Equation

The FEM formulation used as a starting point for this paper is described in [1]. The vector Helmholtz equation can be written in terms of the electric field $\mathbf{E}$ as

$$\nabla \times \left(\frac{\nabla \times \mathbf{E}(\mathbf{r})}{j\omega\mu_0\mu_r} \right) + j\omega\varepsilon_0\varepsilon_r \mathbf{E}(\mathbf{r}) = -\mathbf{J}^{\text{int}}(\mathbf{r}) \qquad (1)$$

where $\mathbf{J}^{\text{int}}(\mathbf{r})$ is the current density of the impressed source. Multiplying (1) by a testing function $\mathbf{w}(\mathbf{r})$ and integrating over the finite element V, one obtains the FEM weak form [10], [11]

$$\int_V \left[\left(\frac{\nabla \times \mathbf{E}(\mathbf{r})}{j\omega\mu_0\mu_r} \right) \cdot (\nabla \times \mathbf{w}(\mathbf{r})) + j\omega\varepsilon_0\varepsilon_r \mathbf{E}(\mathbf{r}) \cdot \mathbf{w}(\mathbf{r}) \right] dV = \int_S (\hat{n} \times \mathbf{H}(\mathbf{r})) \cdot \mathbf{w}(\mathbf{r}) dS - \int_V \mathbf{J}^{\text{int}}(\mathbf{r}) \cdot \mathbf{w}(\mathbf{r}) dV. \qquad (2)$$

Equation (2) can also be derived using a variational method [12].

Manuscript received December 4, 2004; revised March 19, 2005.

C. Guo was with the Department of Electrical and Computer Engineering, University of Missouri-Rolla, Rolla, MO 65409 USA. He is now with Zeland Software, Inc., Fremont, CA 94538 USA.

T. H. Hubing was with the Department of Electrical and Computer Engineering, University of Missouri-Rolla, Rolla, MO 65409 USA. He is now with the Department of Electrical and Computer Engineering, Clemson University, Clemson, SC 29634 USA (e-mail: t.hubing@ieee.org)

Digital Object Identifier 10.1109/TADVP.2006.875089

Within the volume V, the vector tetrahedral elements proposed by Barton and Cendes can be used [13]. The electric field $\mathbf{E}$ within V can be expanded as

$$\mathbf{E}(\mathbf{r}) = \sum_{n=1}^{N} E_n \, \mathbf{w}_n(\mathbf{r}) \tag{3}$$

where N is the total number of interior edges and boundary edges on the dielectric surface, $\{E_n\}$ is a set of unknown complex scalar coefficients, and $\mathbf{w}_n(\mathbf{r})$ is the nth vector basis function.

The surface integral term in (2) can be evaluated using Rao–Wilton–Glisson (RWG) basis functions $\mathbf{f}(\mathbf{r})$ [14]. After multiplying by the testing functions $\mathbf{w}_n(\mathbf{r})$, $n = 1, \ldots, N$, (2) can be written in matrix form as

$$\begin{bmatrix} A_{ii} & A_{is} \\ A_{si} & A_{ss} \end{bmatrix} \begin{bmatrix} E_i \\ E_s \end{bmatrix} = \begin{bmatrix} 0 & 0 \\ 0 & B_{ss} \end{bmatrix} \begin{bmatrix} 0 \\ J_s \end{bmatrix} + \begin{bmatrix} g_i \\ g_s \end{bmatrix} \tag{4}$$

where $\{E_i\}$ is a set of unknowns for the electric field within the FEM volume; $\{E_s\}$ and $\{J_s\}$ are sets of unknowns for the electric field and the electric current density on the surface, respectively; A_{ii}, A_{is}, A_{si}, A_{ss}, and B_{ss} are sparse coefficient matrices; and g_i and g_s are source terms. The elements of $[A]$, $[B]$, and $[g]$ are given by

$$A_{mn} = \int_V \left[\frac{(\nabla \times \mathbf{w}_n(\mathbf{r})) \cdot (\nabla \times \mathbf{w}_m(\mathbf{r}))}{j\omega\mu_0\mu_r} + j\omega\varepsilon_o\varepsilon_r \mathbf{w}_n(\mathbf{r}) \cdot \mathbf{w}_m(\mathbf{r}) \right] dV \tag{5}$$

$$B_{mn} = \int_S \mathbf{w}_m(\mathbf{r}) \cdot \mathbf{f}_n(\mathbf{r}) dS \tag{6}$$

$$g_m^{\text{int}} = -\int_V \mathbf{J}^{\text{int}} \cdot \mathbf{w}_m(\mathbf{r}) dV. \tag{7}$$

B. Equivalent Circuit Equation

The current on the surface can be obtained from the current density as

$$I_{sn} = l_n J_{sn}, \quad n = 1, 2, \ldots, N_s \tag{8}$$

where l_n is the length of nth edge, and N_s is the total number of edges on the boundary surface. I_{sn} represents the current flowing in the direction normal to the nth edge.

The vector basis function associated with the mth edge of a tetrahedron satisfies

$$\mathbf{w}_m(\mathbf{r}) \cdot \mathbf{e}_n(\mathbf{r}) = \delta_{mn}, \text{ for } \mathbf{r} \text{ on the } n\text{th edge} \tag{9}$$

where $\mathbf{e}_n(\mathbf{r})$ is the unit edge vector of the nth edge, $\delta_{mn} = 0$ if $m \neq n$ and $\delta_{mn} = 1$ if $m = n$. The continuity of the tangential electric field along all the edges $\mathbf{E}(\mathbf{r}) \cdot \mathbf{e}_n(\mathbf{r})$ (where $\mathbf{r}$ is on nth edge) $n = 1, 2, \ldots, N$ is ensured in the FEM method. Thus, a voltage can be defined as the electric field circulation along each edge

$$\begin{aligned} V_n &= \int_{\text{edge } n} \mathbf{E}(\mathbf{r}) \cdot \mathbf{e}_n(\mathbf{r}) dl \\ &= \int_{\text{edge } n} \sum_m E_m \mathbf{w}_m(\mathbf{r}) \cdot \mathbf{e}_n(\mathbf{r}) dl = l_n E_n, \\ n &= 1, 2, \ldots, N. \end{aligned} \tag{10}$$

V_n represents the voltage drop along the nth edge.

Using (4)–(8) and (10), the FEM matrix equation can be transformed into circuit equations of the form

$$\begin{bmatrix} Y_{ii} & Y_{is} \\ Y_{si} & Y_{ss} \end{bmatrix} \begin{bmatrix} V_i \\ V_s \end{bmatrix} = \begin{bmatrix} 0 & 0 \\ 0 & K_{ss} \end{bmatrix} \begin{bmatrix} 0 \\ I_s \end{bmatrix} + \begin{bmatrix} I^{\text{int}} \end{bmatrix} \tag{11}$$

where

$$Y_{mn} = \frac{A_{mn}}{l_m l_n} = \frac{1}{j\omega L_{mn}} + j\omega C_{mn} \tag{12}$$

where A_{mn} is defined in (5) and

$$L_{mn} = \frac{\mu_0\mu_r l_m l_n}{\int_V (\nabla \times \mathbf{w}_m(\mathbf{r})) \cdot (\nabla \times \mathbf{w}_n(\mathbf{r})) \, dV} \tag{13}$$

$$C_{mn} = \frac{\varepsilon_0\varepsilon_r}{l_m l_n} \int_V \mathbf{w}_m(\mathbf{r}) \cdot \mathbf{w}_n(\mathbf{r}) dV \tag{14}$$

$$K_{mn} = \frac{B_{mn}}{l_m l_n} \tag{15}$$

$$I_m^{\text{int}} = -\int_V \mathbf{J}^{\text{int}} \cdot \frac{\mathbf{w}_m(\mathbf{r})}{l_m} dV. \tag{16}$$

Equation (11) is analogous to a circuit equation obeying Kirchhoff's current law (KCL), where $[Y_{mn}]$ is a sparse and symmetric admittance matrix. The L_{mn} element in (13) is an inductance term, resulting from the magnetic fields. If ε_r in (14) is a real number, then the C_{mn} element in (14) is a capacitance term, resulting from the electric fields. Notice that both the L_{mn} and C_{mn} terms are independent of frequency. If there is dielectric loss and ε_r is complex, a resistance term can be introduced, as discussed in Section II-C.

When modeling a PCB with closely-spaced power-return plane pairs, the sides of the board can be modeled with four perfect magnetic conductors (PMCs). This PMC boundary condition results in $I_s = 0$, thus (11) can be simplified to

$$\begin{bmatrix} Y_{ii} & Y_{is} \\ Y_{si} & Y_{ss} \end{bmatrix} \begin{bmatrix} V_i \\ V_s \end{bmatrix} = \begin{bmatrix} I^{\text{int}} \end{bmatrix}. \tag{17}$$

Note that the voltages and currents in this equation do not correspond to conventional observable voltages and currents in a power bus structure. However, because they obey Kirchhoff's laws, (17) can be solved using conventional circuit analysis techniques.

C. Equivalent Circuit Network

The currents and voltages can be modeled as port currents and port voltages in a circuit network and (17) can be reformulated as,

$$\begin{bmatrix} Y'_{11} & Y'_{12} & \cdots & Y'_{1n} & \cdots & Y'_{1N} \\ Y'_{21} & Y'_{22} & \cdots & Y'_{2n} & \cdots & Y'_{2N} \\ \vdots & \vdots & \vdots & \vdots & \vdots & \vdots \\ Y'_{m1} & Y'_{m2} & ,\ldots, & Y'_{mn} & \cdots & Y'_{mN} \\ \vdots & \vdots & \vdots & \vdots & \vdots & \vdots \\ Y'_{N1} & Y'_{N2} & \cdots & Y'_{Nn} & \cdots & Y'_{NN} \end{bmatrix} \begin{bmatrix} V_1 \\ V_2 \\ \vdots \\ V_m \\ \vdots \\ V_N \end{bmatrix} = \begin{bmatrix} I^{\text{int}} \end{bmatrix} \tag{18}$$

where the term Y'_{mn} is given by

$$Y'_{mm} = \sum_{n=1}^{N} Y_{mn} = j\omega C'_{mm} + \frac{1}{j\omega L'_{mm}}, \quad m = 1, 2, \ldots, N \tag{19}$$

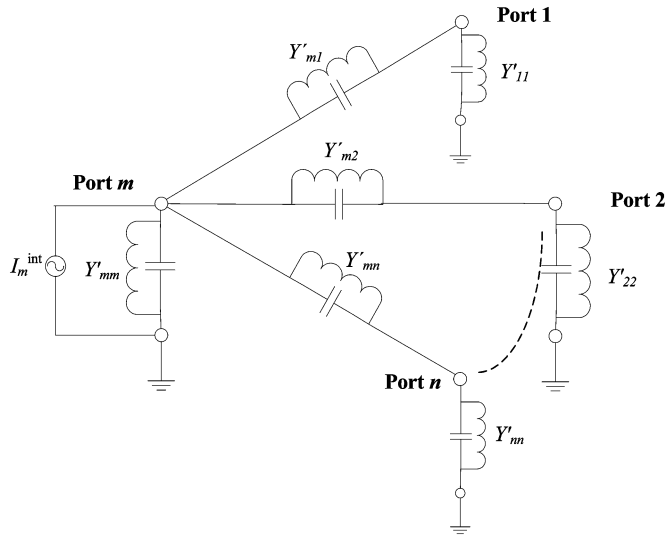

Fig. 1. Equivalent circuit using only passive components.

and the term $Y'_{mn}(m \neq n)$ is given by

$$Y'_{mn} = -Y_{mn}, \quad m \neq n. \tag{20}$$

Fig. 1 shows an equivalent Π network that represents the equivalent circuit looking into Port m in (18). There is one port corresponding to each edge. As indicated in (19), the Y'_{mm} term is a summation of all the Y_{mn} terms on the row corresponding to the mth edge in the matrix $[Y_{mn}]$ of (11), and it is modeled as an inductor in parallel with a capacitor. The $Y'_{mn}(m \neq n)$ terms represent the coupling between Port m and Port n, and are the negative of the off-diagonal terms in the matrix of (11). These terms can also be modeled as inductors in parallel with capacitors.

The circuit network developed in this manner utilizes the symmetric property of the FEM matrix and only requires about half of the circuit components required by the circuit network developed in [9]. Moreover, this network contains only passive components.

Since the matrix $[Y_{mn}]$ is sparse, there are a limited number of ports that couple to Port m. A typical value for the number of nonzero elements for the matrix $[Y_{mn}]$ is about 10 to 20 elements per row. Thus, the number of circuit components required to build the circuit network is only proportional to N.

III. PCB Power Bus Modeling

Power bus structures in real PCBs exhibit losses due to the finite resistance of the conductor walls and the dielectric loss. These losses can be readily incorporated into the circuit models described in the previous section.

A. Dielectric Loss

Dielectric materials may dissipate some electromagnetic energy in the form of heat. This loss can be characterized by a loss tangent δ, and the relative permittivity of the dielectric is given by

$$\varepsilon_r = \varepsilon'_r - j\varepsilon''_r = \varepsilon'_r(1 - j\tan\delta) = \varepsilon'_r\left(1 - j\frac{\sigma}{\omega\varepsilon'_r}\right). \tag{21}$$

Both ε'_r and σ are generally functions of frequency; however, for most printed circuit board materials, the loss tangent is relatively constant over a wide range of frequencies.

Substituting (21) into (5), the elements of the admittance matrix $[Y_{mn}]$ in (11) are given by

$$Y_{mn} = \frac{1}{j\omega L_{mn}} + j\omega C_{mn} + \frac{1}{R_{mn}} \tag{22}$$

where

$$R_{mn} = \frac{l_m l_n}{\omega\varepsilon_0 \tan\delta \int_V \mathbf{w}_m(\mathbf{r}) \cdot \mathbf{w}_n(\mathbf{r}) dV}. \tag{23}$$

Equation (19) and (20) can still be used to develop an equivalent circuit that now includes resistors. However, notice that R_{mn} is inversely proportional to the frequency.

B. Conductor Loss

The finite conductivity of the power planes can be modeled using the FEM method by applying an impedance boundary condition. The resulting FEM matrix equation is given by [15]

$$\begin{bmatrix} A_{ii} & A_{ik} & A_{is} \\ A_{ki} & A_{kk} + S_{kk} & A_{ks} \\ A_{si} & A_{sk} & A_{ss} \end{bmatrix} \begin{bmatrix} E_i \\ E_k \\ E_s \end{bmatrix} = \begin{bmatrix} g^{\text{int}} \end{bmatrix} \tag{24}$$

where the coefficients $[\mathbf{E}_k]$ are a set of unknowns for the impedance boundary edges, the elements of the $[A]$ matrix are given by (5). The elements of the submatrix S_{kk} are given by

$$S_{mn} = \int_{S_k} \frac{1}{\eta_S} \mathbf{f}_m(\mathbf{r}) \cdot \mathbf{f}_n(\mathbf{r}) dS \tag{25}$$

where the surface impedance η_S on impedance surface S_k is given by

$$\eta_S = (1+j)R_S = (1+j)\left(\frac{1}{\sigma\delta}\right) = (1+j)\sqrt{\frac{\pi f \mu_0}{\sigma}}. \tag{26}$$

For a perfect electric conductor (PEC), $E_k = 0$, so these terms do not appear in (4). Thus, the order of (24) is always larger than that of (4) when used to analyze the same structure.

We can also define a voltage V_k associated with E_k, and the corresponding circuit equation is given by

$$\begin{bmatrix} Y_{ii} & Y_{ik} & Y_{is} \\ Y_{ki} & Y_{kk} + G_{kk} & Y_{ks} \\ Y_{si} & Y_{sk} & Y_{ss} \end{bmatrix} \begin{bmatrix} V_i \\ V_k \\ V_s \end{bmatrix} = \begin{bmatrix} I^{\text{int}} \end{bmatrix} \tag{27}$$

where the elements Y_{mn} are given by (12) and the elements G_{mn} are given by

$$G_{mn} = \frac{1}{\eta_S l_m l_n} \int_{S_k} \mathbf{f}_m(\mathbf{r}) \cdot \mathbf{f}_n(\mathbf{r}) dS \tag{28}$$

which can be further decomposed into

$$\begin{aligned} G_{mn} &= G'_{mn} - jG''_{mn} \\ &= \frac{\int_{S_k} \mathbf{f}_m(\mathbf{r}) \cdot \mathbf{f}_n(\mathbf{r}) dS}{2R_S l_m l_n} - j\frac{\int_{S_k} \mathbf{f}_m(\mathbf{r}) \cdot \mathbf{f}_n(\mathbf{r}) dS}{2R_S l_m l_n}. \end{aligned} \tag{29}$$

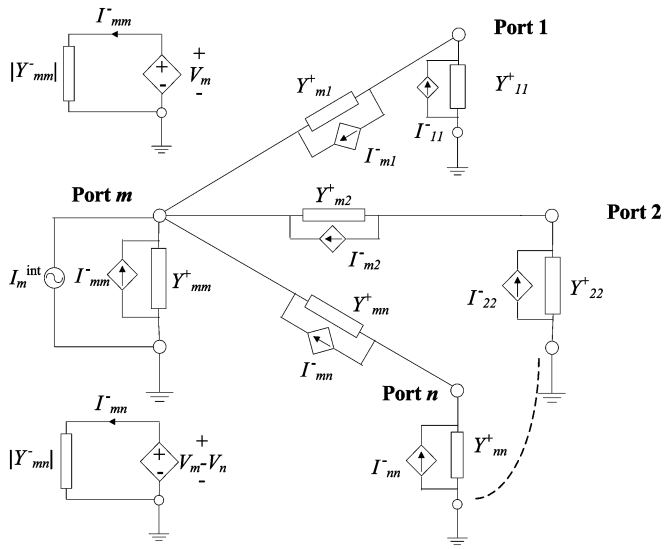

Fig. 2. Equivalent circuit using active sources.

Notice that R_S is normally frequency dependent, so the G'_{mn} term can be modeled using a frequency-dependent resistor, and G''_{mn} can be modeled using a frequency-dependent inductor.

C. Negative-Valued Components

The circuit network with only passive components shown in Fig. 1 may not always be practical, since the passive circuit components L_{mn}, C_{mn} (or R_{mn} when loss is considered) may have negative values. Some implementations of SPICE may not accept components with negative values. For a frequency-domain analysis (*ac analysis* in SPICE), the SPICE program we used (HSPICE) works fine with negative-valued components. In this case, the circuit network shown in Fig. 1 is optimal due to the small number of circuit components.

For a time-domain analysis (*transient analysis* in SPICE), circuit components with negative values may result in stability issues. Dependent sources can be introduced to change the current-voltage relationship of components with negative values, so that only components with positive values are used throughout the entire network. Such an equivalent network is shown in Fig. 2.

In this circuit representation, the components with positive values in the admittance term Y'_{mm} and $Y'_{mn}(m \neq n)$ are given by Y^+_{mm} and $Y^+_{mn}(m \neq n)$, respectively. If there are components with negative values in the admittance term Y'_{mm}, denoted as Y^-_{mm}, or in the admittance $Y'_{mn}(m \neq n)$, denoted as $Y^-_{mn}(m \neq n)$, current-controlled current sources I^-_{mm} and $I^-_{mn}(m \neq n)$ are introduced. The circuits for the controlling currents are also shown in Fig. 2, where voltage-controlled voltage sources are used and the components with negative values have been changed into those with positive values. In practice, dependent sources are only required to represent the elements with negative values. Positive-valued components can still be represented by passive elements as shown in Fig. 1.

D. Quasi-Static Solution

Since the electromagnetic wave equation used to derive the FEM equations cannot be used to solve quasistatic electric or magnetic field problems, the equivalent circuit network derived using FEM-SPICE should not be expected to work at low frequencies either. However, when modeling power bus structures, the summation of the capacitance terms C'_{mm} in (19) ($m = 1, 2, \ldots, N$) is equal to the capacitance of the parallel plate capacitor formed by the power-return plane pairs and dielectric. The maximum energy stored in the electric field is given by

$$W_E = \int_V w_e dV = \int_V \frac{1}{2}\varepsilon \left|\mathbf{E}(\mathbf{r})\right|^2 dV. \tag{30}$$

Substituting (3) into (30), W_E can be expressed as

$$\begin{aligned} W_E &= \int_V \frac{1}{2}\varepsilon_0\varepsilon_r \left[\sum_{m=1}^{N} E_m \boldsymbol{w}_m(\boldsymbol{r})\right] \cdot \left[\sum_{n=1}^{N} E_n \boldsymbol{w}_n(\boldsymbol{r})\right] dV \\ &= \int_V \frac{1}{2}\varepsilon_0\varepsilon_r \sum_{m=1}^{N}\sum_{n\in\Delta_m} E_m E_n \boldsymbol{w}_m(\boldsymbol{r})\cdot\boldsymbol{w}_n(\boldsymbol{r}) dV \\ &= \frac{1}{2}\sum_{m=1}^{N}\sum_{n\in\Delta_m} E_m E_n \int_V \varepsilon_0\varepsilon_r \left[\boldsymbol{w}_m(\boldsymbol{r})\cdot\boldsymbol{w}_n(\boldsymbol{r})\right] dV. \end{aligned} \tag{31}$$

From (14) and (19), (31) can be rewritten as

$$\begin{aligned} W_E &= \frac{1}{2}\sum_{m=1}^{N}\sum_{n\in\Delta_m} E_m E_n l_m l_n C_{mn} \\ &= \frac{V^2}{2}\sum_{m=1}^{N}\sum_{n\in\Delta_m} C_{mn} = \frac{V^2}{2}\sum_{m=1}^{N} C'_{mm} \end{aligned} \tag{32}$$

where V is the voltage between the power and return planes. The total electric energy can also be given by $W_E = C_b V^2/2$, where C_b is the capacitance of the parallel plate capacitor formed by the power-return plane pairs and dielectric. Therefore, the summation of the capacitance terms C'_{mm} is equal to C_b, and the solution at very low frequencies is obtained by neglecting all components in the circuit except the capacitors between nodes on the upper and lower plates.

In practice, the software implementation of this analysis technique places an inductor in parallel with a capacitor between every pair of connected nodes. The inductors between nodes on the upper and lower plates have very large values, but they are not infinite due to discretization error. At very low frequencies, these inductors effectively short the top and bottom plates, producing erroneous results. By simply eliminating the large-valued inductors from the analysis, excellent results are achieved when modeling power bus structures at arbitrarily low frequencies using the FEM-SPICE method.

IV. Numerical Examples

A typical rectangular power bus structure is shown in Fig. 3. The board dimensions are $L \times W \times h$. The top and bottom planes are conductors. The dielectric between the conductor layers has a relative dielectric constant of ε_r and a loss tangent of $\tan\delta$. An ideal current source is used to excite the structure at the point (x_i, y_i).

The first sample problem is to model the input impedance of the rectangular power bus structure with dielectric loss where $L = 5$ cm, $W = 4$ cm, $h = 2$ mm, $\varepsilon_r = 4.2$, $\tan\delta = 0.02$ (FR-4), and the current source is located at $x_i = 2$ cm and

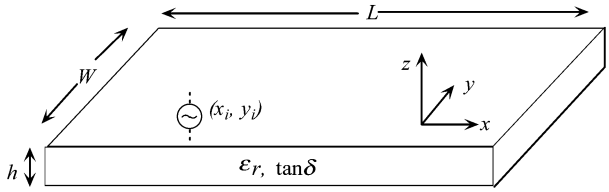

Fig. 3. Typical rectangular power bus structure.

TABLE I
PARAMETERS OF THE EQUIVALENT CIRCUIT NETWORK FOR PROBLEM 1

	Passive network (Fig. 1)	Active network (Fig. 2)	The network in [9]
# of tetrahedrons	1178		
# of FEM edges (# of circuit ports)	841		
# of circuit nodes	3648	8984	17678
# of circuit components	12907	20911	41807
Simulation time (sec)	140	271	717

$y_i = 1$ cm. The top and bottom planes are modeled as PECs. Discretization parameters are listed in Table I. The equivalent circuit network shown in Fig. 1 with resistors added to model the dielectric loss was used. The network shown in Fig. 2 and the network given in [9] were also generated for comparison. The solution time is the total time for HSPICE to do an ac analysis from 1 MHz linearly increasing to 5 GHz in 500 frequency steps. As we can see, the network in Fig. 1 requires the least number of circuit components and the least computational effort. The equivalent network in Fig. 2 requires approximately twice the number of circuit components and solution time. The network in [9] requires the most computational effort because it does not take advantage of the symmetric property of the FEM matrix.

The input impedance of the power bus structure can also be calculated using a cavity model. Cavity models determine the input impedance by summing the contributions of all relevant resonant cavity modes as

$$Z_{\text{in}} = j\varpi\mu h \sum_{m=0}^{M}\sum_{n=0}^{N} \frac{\chi_{mn}^2 \cos^2(k_{xm}x_s)\cos^2(k_{yn}y_s)}{ab\left(k_{xm}^2 + k_{yn}^2 + \gamma^2\right)} \quad (33)$$

where M and N are positive integers that are sufficiently large to converge to the correct solution. A more detailed explanation of (33) can be found in [6].

Fig. 4 compares the FEM-SPICE result using the network in Fig. 1 with the cavity model result. The same boundary conditions were used in both methods. The results agree within 1 dB up to 5 GHz.

Problem 2 is a rectangular power bus structure where the conductor loss is dominant. The board dimensions are $L = 12$ mm, $W = 10$ mm, and $h = 0.4$ mm. In order to exaggerate the conductor loss, the dielectric is assumed to be lossless with $\varepsilon_r = 21.5$, and the conductivity of the top and bottom planes is 7.0×10^4 S/m (e.g., graphite). The current source is located at $x_i = 4$ mm and $y_i = 3$ mm. For this problem, the equivalent circuit network shown in Fig. 1 with resistors and inductors added to impedance boundary edges to model conductor loss were used, as shown in Fig. 5. Port m corresponds to an impedance

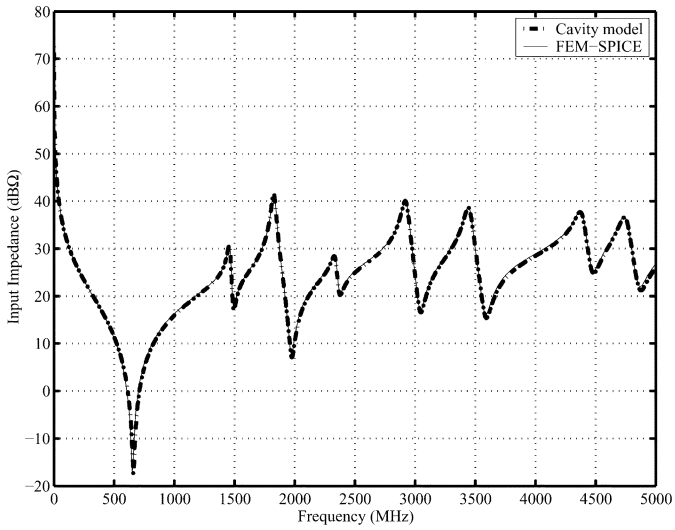

Fig. 4. Calculated input impedance using cavity model and FEM-SPICE for Problem 1.

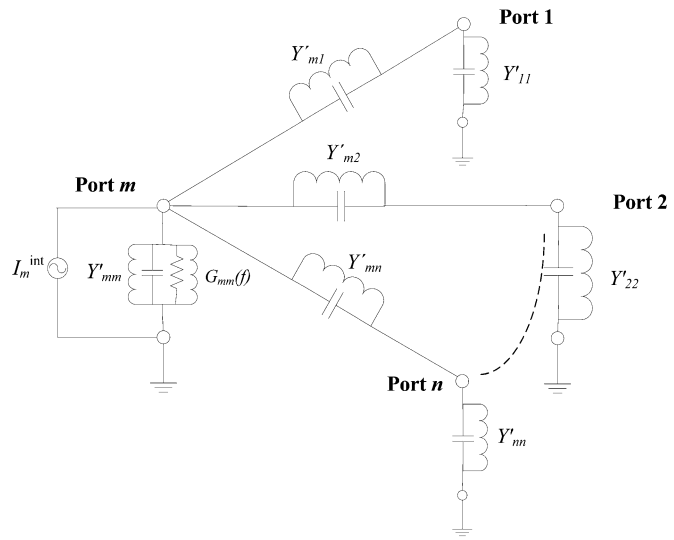

Fig. 5. Equivalent circuit with components to model conductor loss.

TABLE II
PARAMETERS OF THE EQUIVALENT CIRCUIT NETWORK FOR PROBLEM 2

# of tetrahedra	# of circuit ports	# of circuit nodes	# of circuit components	Simulation time (sec)
1211	2122	21260	55058	5423

boundary edge. Discretization parameters for the equivalent circuit network are shown in Table II.

Even though this board is much smaller than the board in Problem 1, it requires about the same number of tetrahedra. The smaller height forces the dimensions of each tetrahedron to be small in order to maintain a proper aspect ratio. The complexity of the circuit network almost doubles and more computation is required due to the large number of frequency-dependent resistors and inductors necessary to model the impedance boundary condition. The calculated input impedance using FEM-SPICE is compared to cavity model results in Fig. 6. The results agree within a few decibels at all frequencies evaluated.

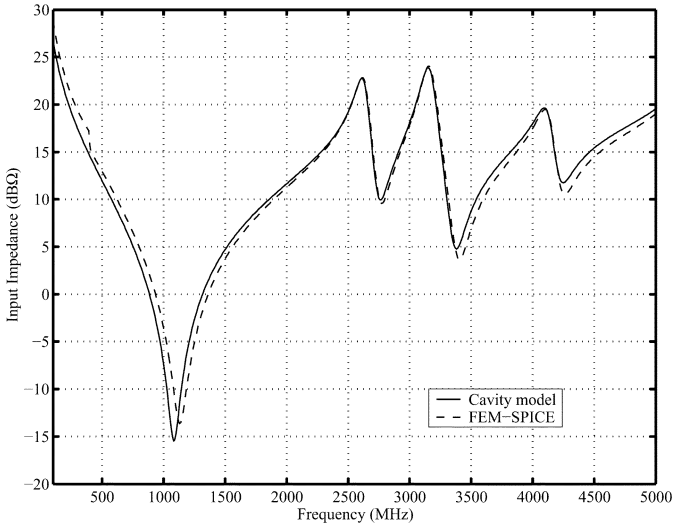

Fig. 6. Calculated input impedance using cavity model and FEM-SPICE for Problem 2.

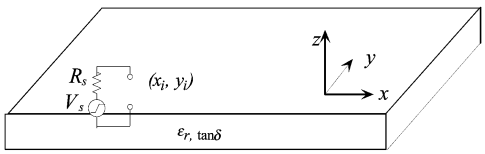

Fig. 7. The excitation for transient analysis in Problem 3.

Problem 3 demonstrates the ability to perform a transient analysis using the circuit network developed from the FEM-SPICE method. The same board used in the first problem is analyzed. This time the equivalent circuit network in Fig. 2 is used to do the analysis. The equivalent circuit network in Fig. 1 is simpler; however, some elements have negative values, which can result in instability when using HSPICE. The circuit network in [9] was not evaluated due to its complexity. The source used to drive the power bus structure is shown in Fig. 7. The rise time of the voltage source V_s is about 50 ps. The source impedance R_s is 50 Ω.

The cavity model can also be used to generate an equivalent circuit network for the power bus structure. The step response of the power bus structure calculated using networks generated from FEM-SPICE and the cavity model are shown in Fig. 8. As we expect, the response calculated using the FEM-SPICE model agrees well with that of the equivalent circuit generated using the cavity model.

Problem 4 is to analyze a power bus structure of irregular shape. The top and bottom planes are assumed to be PECs. Their shape is that of a rectangle combined with half of a circle as shown in Fig. 9. The dielectric parameters are $\varepsilon_r = 4.2$ and $\tan\delta = 0.02$ (FR-4). An ideal current source is located at $x_i =$ 3 cm and $y_i = 2$ cm.

For such an irregular structure, it is difficult to derive an analytical solution using a cavity model. To validate the input impedance calculated using FEM-SPICE, commercial FEM software (Ansoft HFSS) was also used to analyze this structure. The calculated results are shown in Fig. 10. The results agree within 2 dB at all frequencies evaluated.

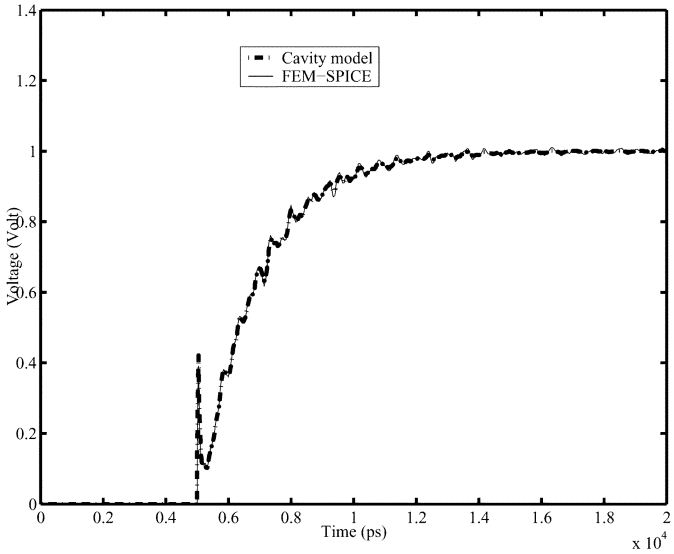

(a) Step response up to 20 ns

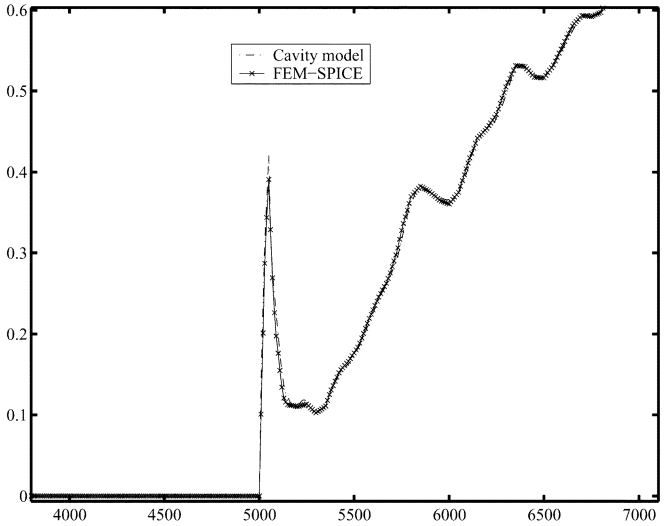

(b) Closer view of the step response

Fig. 8. Step-response of the power bus structure calculated from a cavity model and FEM-SPICE.

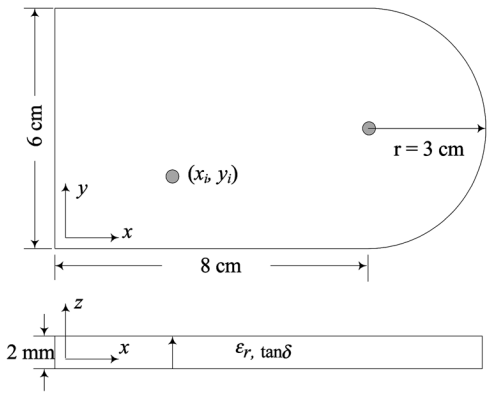

Fig. 9. Irregular power bus structure in Problem 4.

V. Conclusion

The FEM-SPICE method presented in this paper can be used to derive equivalent circuit models for three-dimensional

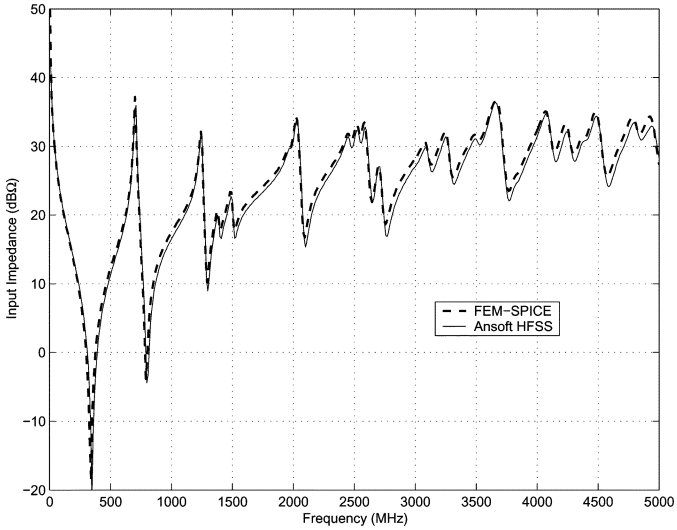

Fig. 10. Calculated input impedance for Problem 4.

electromagnetic geometries. These models can then be analyzed using SPICE-like circuit solvers in the time or frequency domains.

This technique is particularly well suited for modeling printed circuit board power bus structures from dc to several gigahertz. Unlike traditional circuit-based models for printed circuit boards based on lumped element grids, the FEM-SPICE method provides a full-wave solution. And unlike other full-wave circuit-based methods, the method presented here generates sparser matrices and is capable of modeling both conductor and dielectric losses.

Two circuit formulations were derived. The first consists entirely of passive components. This formulation is the most efficient and can be used for frequency domain simulations. However, some of the component values may be negative, which may create stability problems when performing a time-domain simulation. The second formulation derived employs dependent sources to convert components with negative values to components with positive values.

REFERENCES

[1] Y. Ji and T. Hubing, "EMAP5: A 3-D hybrid FEM/MoM code," *Appl. Computat. Electromagn. Soc. J.*, vol. 15, no. 1, pp. 1–12, Mar. 2000.

[2] S. Van der Berghe, F. Olyslager, D. De Zutter, J. De Moerloose, and W. Temmerman, "Study of the ground bounce caused by power plane resonances," *IEEE Trans. Electromagn. Compat.*, vol. 40, no. 2, pp. 111–119, May 1998.

[3] A. E. Ruehli, "Equivalent circuit models for three-dimensional multiconductor systems," *IEEE Trans. Microw. Theory Tech.*, vol. MTT-22, no. 3, pp. 216–221, Mar. 1974.

[4] Y. T. Lo, D. Solomon, and W. F. Richards, "Theory and experiment on microstrip antennas," *IEEE Trans. Antennas Propagat.*, vol. AP-27, no. 2, pp. 137–145, Mar. 1979.

[5] N. Na, J. Choi, S. Chun, M. Swaminathan, and J. Srinivasan, "Modeling and transient analysis of planes in electronic packages," *IEEE Trans. Adv. Packag.*, vol. 23, no. 3, pp. 340–352, Aug. 2000.

[6] M. Xu and T. Hubing, "Estimating the power bus impedance of printed circuit boards with embedded capacitance," *IEEE Trans. Adv. Packag.*, vol. 25, no. 3, pp. 424–432, Aug. 2002.

[7] K. Guillouard, M.-F. Wong, V. F. Hanna, and J. Citerne, "A new global finite-element analysis of microwave circuits including lumped elements," *IEEE Trans. Microw. Theory Tech.*, vol. 44, no. 12, pp. 2587–2594, Dec. 1996.

[8] M. Feliziani and F. Maradei, "FEM solution of time-harmonic electromagnetic fields by an equivalent electrical network," *IEEE Trans. Magn.*, vol. 36, no. 4, pp. 938–941, Jul. 2000.

[9] ——, "Circuit-oriented FEM: Solution of circuit-field coupled problems by circuit equations," *IEEE Trans. Magn.*, vol. 38, no. 2, pp. 965–968, Mar. 2002.

[10] A. Peterson, S. Ray, and R. Mittra, *Computational Methods for Electromagnetics*. New York: IEEE Press, Oxford Univ. Press, 1997, pp. 461–463.

[11] P. P. Silvester and R. L. Ferrari, *Finite Elements for Electrical Engineers*, 3rd ed. New York: Cambridge Univ. Press, 1996, pp. 405–406.

[12] J.-M. Jin, *The Finite Element Method in Electromagnetics*. New York: Wiley, 1993.

[13] M. L. Barton and Z. J. Cendes, "New vector finite elements for three-dimensional magnetic field computation," *J. Appl. Phys.*, vol. 61, pp. 3919–3921, Apr. 1987.

[14] S. M. Rao, D. R. Wilton, and A. W. Glisson, "Electromagnetic scattering by surfaces of arbitrary shape," *IEEE Trans. Antennas Propagat.*, vol. AP-30, no. 3, pp. 409–418, May 1982.

[15] H. Wang, M. Xu, C. Wang, and T. Hubing, "Impedance boundary conditions in a hybrid FEM/MOM formulation," *IEEE Trans. Electromagn. Compat.*, vol. 45, no. 2, pp. 198–206, May 2003.

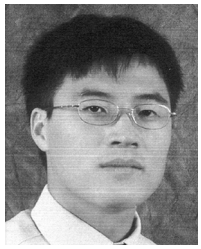

Chunlei Guo (M'05) received the B.S. and M.S. degrees in electrical engineering from Tsinghua University, Beijing, China, and the Ph.D. degree in electrical engineering from the University of Missouri, Rolla, in 1998, 2000, and 2005, respectively.

He is currently with Zeland Software, Inc, Fremont, CA. His interests include the development and application of computational electromagnetic techniques for analyzing antennas, signal integrity, and electromagnetic compatibility problems.

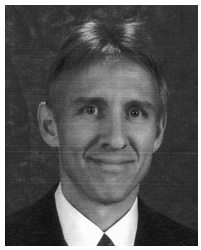

Todd H. Hubing (F'06) received the B.S. degree in electrical engineering from the Massachusetts Institute of Technology, Cambridge, in 1980, the M.S. degree in electrical engineering from Purdue University, West Lafayette, IN, in 1982, and the Ph.D. degree in electrical engineering from North Carolina State University, Raleigh, in 1988.

From 1982 to 1989, he was with the Electromagnetic Compatibility Laboratory, IBM Communications Products Division, Research Triangle Park, NC. In 1989, he decided that he wanted to spend less time fixing EMC problems and more time trying to understand them, so he left IBM to start an EMC Laboratory at the University of Missouri-Rolla (UMR). At UMR, he worked with faculty and students to analyze and develop solutions for a wide range of EMC problems affecting the electronics industry. In 2006, he joined Clemson University, Clemson, SC, as the Michelin Professor for Vehicular Electronics. There, he is continuing his work in electromagnetic compatibility and computational electromagnetic modeling, particularly as it applies to automotive and aerospace electronic systems.

Prof. Hubing has served as an Associate Editor of the IEEE TRANSACTIONS ON ELECTROMAGNETIC COMPATIBILITY, the IEEE EMC Society Newsletter, and the *Journal of the Applied Computational Electromagnetics* Society. He has served on the board of directors for both the Applied Computational Electromagnetics Society and the IEEE EMC Society. He was the 2002-2003 President of the IEEE EMC Society.